Astron. Astrophys. 350, 840–846 (1999)

ASTRONOMY AND ASTROPHYSICS

HST observations of Terzan 1: a second parameter globular cluster in the galactic bulge⋆

S. Ortolani[1,2], B. Barbuy[3], E. Bica[4], A. Renzini[2], G. Marconi[5], and R. Gilmozzi[2]

[1] Università di Padova, Dipartimento di Astronomia, Vicolo dell'Osservatorio 5, 35122 Padova, Italy (ortolani@pd.astro.it)
[2] European Southern Observatory, Karl-Schwarzschild-Strasse 2, 85748 Garching bei München, Germany (sortolan,arenzini,rgilmozz@eso.org)
[3] Universidade de São Paulo, CP 3386, São Paulo 01060-970, Brazil (barbuy@orion.iagusp.usp.br)
[4] Universidade Federal do Rio Grande do Sul, Dept. de Astronomia, CP 15051, Porto Alegre 91501-970, Brazil (bica@if.ufrgs.br)
[5] Osservatorio Astronomico di Roma, Via dell'Osservatorio 2, 00040 Monteporzio, Italy (marconi@mporzio.astro.it)

Received 1 July 1999 / Accepted 3 September 1999

Abstract. Hubble Space Telescope observations in the F555W and F814W bands are presented of the bulge globular cluster Terzan 1. This highly obscured cluster has the smallest projected distance to the Galactic center among all known globulars. Its colour-magnitude diagram shows a red horizontal branch, which is typical of metal-rich clusters, combined to a very steep red giant branch, which instead is typical of metal-poor clusters. These features make it similar to the second parameter halo cluster NGC 362. Terzan 1 is therefore another second parameter cluster in the Galactic bulge, and the first one in the bulge combining a steep red giant branch with a red horizontal branch. As in the case of NGC 362, these features of the colour-magnitude diagram can be accounted for by the cluster being $\sim$ 2 Gyr younger than other clusters with the same metallicity but showing a blue horizontal branch. These findings demonstrate that second parameter effects are not confined to the Galactic halo, but are actually encountered at all galactocentric distances. Despite the unusual sequences in the colour-magnitude diagram, the derivation of reddening and distance is straightforward, and we obtained $E(B-V) = 2.48 \pm 0.1$, $d_{\odot} = 5.2 \pm 0.5$ kpc, thus placing Terzan 1 within the bulge.

Key words: stars: Hertzsprung–Russel (HR) and C-M diagrams – Galaxy: globular clusters: individual: Terzan 1

1. Introduction

Of the $\sim$ 150 globular clusters (GC) belonging to the Milky Way, $\sim$ 70 lie within $\sim$ 4 kpc from the galactic center where the density of GCs tends to peak. While some of these clusters may be in elongated orbits and are now caught near their perigalacticon, the vast majority of them belong to the Galactic bulge, as they share the kinematical properties and metallicity distribution of bulge stars (e.g. Minniti 1995). These bulge GCs are therefore useful tracers for the study of the bulge itself, especially for determining the age of the bulge stellar population, and provide clues about the formation, chemical enrichment, and evolution of the bulge itself (e.g. Barbuy et al. 1998). Some of these GCs are highly obscured by dust in the galactic disk and/or lie in very crowded regions which makes them prime targets for HST observations aimed at constructing accurate colour-magnitude diagrams (CMD).

HST/WFPC2 observations of two metal-rich bulge GCs (namely, NGC 6528 and NGC 6553) have allowed us to demonstrate that their age must be very close to that of the inner halo GC 47 Tuc, hence that the bulge underwent a very rapid chemical enrichment, early in the evolution of the Milky Way (Ortolani et al. 1995). Moreover, in the same study a comparison of the luminosity function of these clusters to that of the bulge in Baade's Window ($\sim 4^{\circ}$ from the galactic center) allowed us to exclude the presence of a significant intermediate age population in the bulge itself.

As part of the same project, HST data were also collected for the highly reddened cluster Terzan 1, which is the globular cluster with smallest projected distance ($2^{\circ}.7$) to the Galactic center (Terzan 1968; Ortolani et al. 1993a).

In the present paper we provide deep HST optical photometry for Terzan 1 which attains the main sequence turnoff. Over the previous ground based observations (Ortolani et al. 1993a), the HST CMD shows a much improved definition of the bright evolutionary sequences, but also reveals puzzling features indicative of a *second parameter* effect. This effect consists in the poor correlation of horizontal branch (HB) morphology with metallicity, and is widespread among halo clusters. Nevertheless, Lee et al. (1994) found no evidence of a second parameter effect among GCs with galactocentric distance less than $\sim$ 8 kpc, and argued this effect to be confined to the outer halo of the Galaxy. However, HST observations of two metal-rich clusters belonging to the Galactic bulge (NGC 6388 and NGC 6441) showed the presence of a substantial blue extension of the HB, a clear second parameter effect (Rich et al. 1997).

Send offprint requests to: B. Barbuy

⋆ Observations obtained at the Space Telescope Science Institute, with the NASA/ESA Hubble Space Telescope, operated by AURA Inc. under contract to NASA

Table 1. Metallicity values of Terzan 1 from the literature

[Fe/H]	reference	method
+0.24	1	integrated IR photometry
–0.71	2	CaII T integrated spectroscopy
> 0.0	3	CMDs
+0.03	4	IR CO bands integrated spectroscopy
–0.18	5	CaII T integrated spectroscopy

References: 1: Zinn & West (1984) based on Malkan's (1982) infrared photometry; 2: Armandroff & Zinn (1988); 3: Ortolani et al. (1991, 1993a); 4: Origlia et al. (1997); 5: Bica et al. (1998).

We now provide evidence suggesting that Terzan 1 may be yet a third example of a second parameter cluster in the Galactic bulge. Its HB consists dominantly of red stars, contrary to the dominant correlation of HB morphology with metallicity as indicated by the slope of the red giant branch (RGB).

In Sect. 2 we report about previously known properties of this cluster, while in Sect. 3 the HST observations and subsequent reductions are described. In Sect. 4 the CMDs in the various WFPC2 frames are presented and some cluster parameters are derived from them. In Sect. 5 possible scenarios are discussed to account for the anomalous CMD of this cluster, and finally our concluding remarks are given in Sect. 6.

2. Cluster parameters

Terzan 1 is also known as HP2, GCL 69, GCL B1732-3027, ESO455-SC23 and has coordinates (α_{1950} = $17^{\rm h}32^{\rm m}34^{\rm s}$ and δ_{1950} = –30°27′00″ (l = 357.56°, b = 0.99°). The cluster shows a post-core collapse structure (Trager et al. 1995).

2.1. Metallicity

The metallicity is a crucial parameter for the interpretation of the cluster CMD. In Table 1 are reported [Fe/H] values for Terzan 1 as derived from the literature. All estimates point to a fairly high metallicity, although ranging from the level of 47 Tuc ([Fe/H] = –0.7) to above solar. It should be noted, however, that no high resolution spectroscopy of individual stars is yet available, and therefore only integrated-light methods have been used. The large spread among values in Table 1 is likely to arise from various contamination effects. In fact, within a radius of $10''$ from the cluster center there is a bright field foreground M giant (Bica et al. 1998) which is clearly seen near the lower left corner in Fig. 1, and at least two bright disk blue stars (Bica et al. 1993). Moreover, due to its low galactic latitude the cluster is highly reddened and is projected over a field of high stellar density, with stars belonging both the the disk and the bulge. The contaminating stars affect in different ways the results depending on the aperture used in the various studies, as well as on the scanning and extraction techniques, and on the spectral region used in deriving the cluster metallicity. Decontamination from the light of stars that are not cluster members is therefore rather difficult and uncertain.

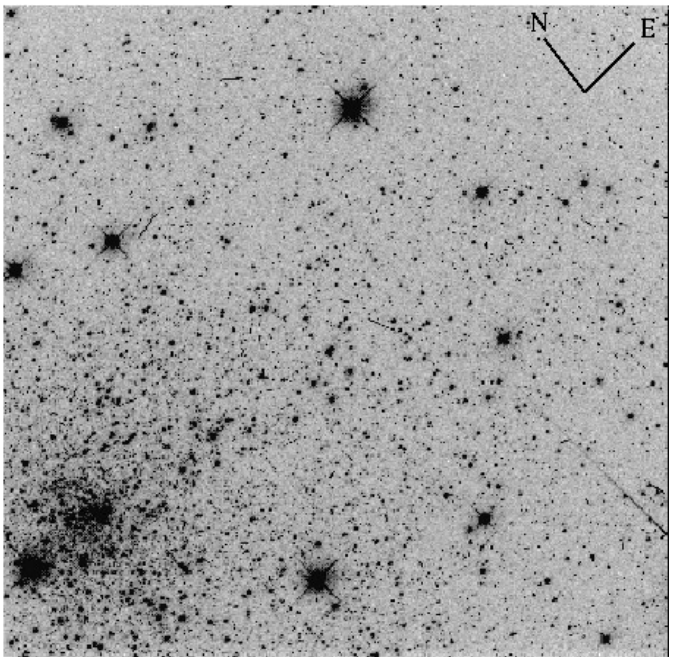

Fig. 1. WFPC2 W3 500 sec F555W image which contains the cluster center. North is to the upper left corner and East is to the upper right corner.

The two bright blue stars may have diluted the blue spectral region, reducing the CaII triplet equivalent width, and therefore leading to the lower metallicity value estimated by Armandroff & Zinn (1988). Malkan's (1982) integrated infrared photometry, on which Zinn & West (1984) based their estimate, provided the highest metallicity value, and might have been affected by the contamination of light from the M giant.

Origlia et al.'s (1997) integrated spectroscopy in the *H* band sampled a $4\farcs4 \times 6\farcs6$ area centered on the cluster, apparently excluding the bright foreground M giant, while the blue stars should have little effect on the infrared measurements. Their observations indicate a strong CO band, which therefore should be representative of the cluster stars.

The near-IR integrated spectra in Bica et al. (1998) sample a large area ($90'' \times 10''$) and should represent as much as possible the cluster global properties. The pixels corresponding to the M giant were excluded from the analyzed spectrum. Their CaII triplet is stronger than that of Armandroff & Zinn (1988). Finally, Ortolani et al. (1991, 1993a) argued for a high metallicity from the red HB exhibited by the CMD obtained from ground-based observations.

2.2. Reddening

Literature values for the reddening in front of Terzan 1 scatter over a rather wide range, and have been derived using a variety of methods (Table 2). Like for the metallicity, this spread is likely to arise mostly from contamination effects by field stars, which affect the results in different ways depending on the adopted method. In Sect. 4 we shall derive a new value of the reddening using the HST data themselves.

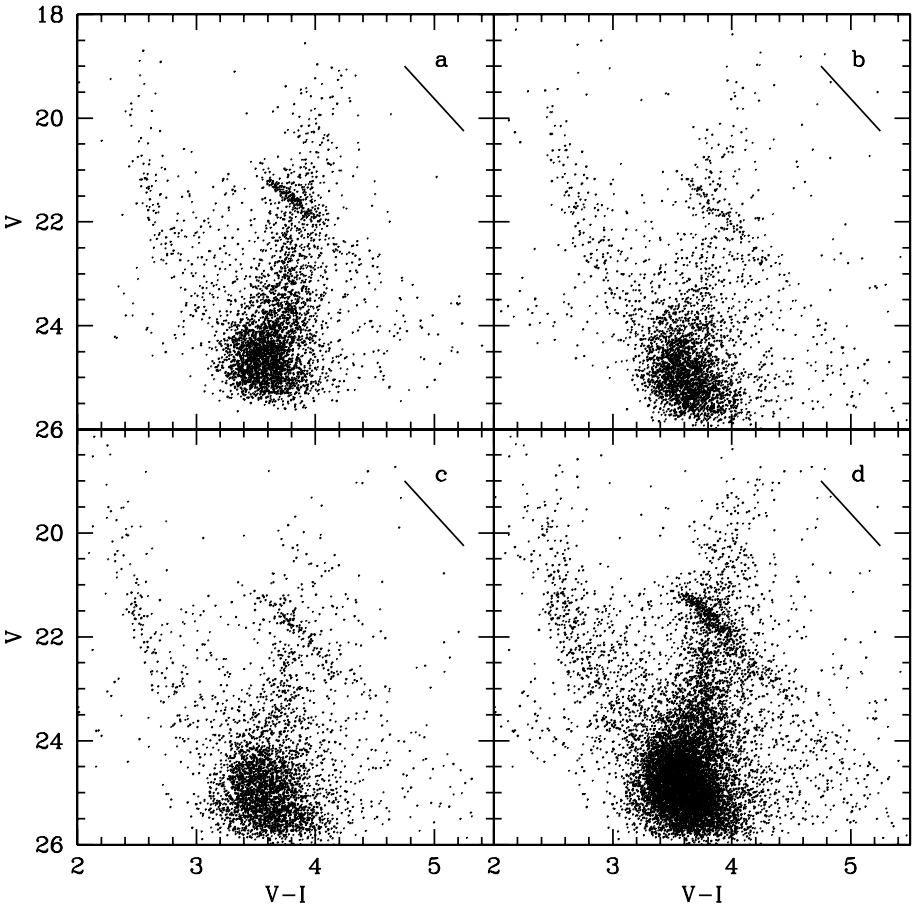

Fig. 2a–d. V vs. (V-I) CMDs for the individual wide-field cameras ($80'' \times 80''$), and combined diagrams. **a** W3 which contains the cluster center; **b** W2; **c** W4; **d** W2+W3+W4.

Table 2. Reddening of Terzan 1 given in the literature

$E(B-V)$	reference	method
1.50	1	integrated IR photometry
1.52	2	compilation
1.49	3	near-IR spectroscopy
1.64	4	compilation
2.04	5	compilation
1.67	6	CMDs
1.80	7	integrated near-IR spectroscopy

References: 1: Malkan (1982); 2: Webbink (1985); 3: Armandroff & Zinn (1988); 4: Harris (1996); 5: Peterson 1993; 6: Ortolani et al. (1993a); 7: Bica et al. (1998).

3. Observations and reductions

Terzan 1 was observed with HST/WFPC2 on 1994 February 25, through the F555W (V) and F814W (I) filters. The cluster center was placed near the corner of the W3 chip (see Fig. 1) and the telescope was kept in the same position during all the exposures. Two 500 s exposures were taken through the F555W filter, followed by a 30 s exposure in the same filter. Two 60 s exposures and one 5 s exposure were obtained through F814W filter. The average images have been reduced with DAOPHOT II, and calibrated using the synthetic equations given by Holtzman et al. (1995), as in their Table 10, because the empirical equations do not cover our $V-I$ colour range. As explained by these authors, the appropriate calibration for reddened objects would be to correct the instrumental magnitudes for reddening, to apply the calibration-transformation to the standard Johnson-Cousins system, and finally correct for reddening back in the Johnson-Cousins transformed photometry. However, since Terzan 1 reddening is not well-known, we decided to apply directly the transformation-calibration to the original data. From Holtzman et al. it appears that this procedure should introduce only marginal deviations in the case of the filters used in the present study.

According to Trager et al. (1995), the half light radius is $r_{\rm h} = 229''$, and 20% of the cluster light is within the radius $r_{20} = 81''$. The WFPC2 frames therefore sample $\sim 20\%$ of the total cluster light. Notice that the concentration of stars evident in Fig. 1 corresponds to just the cluster core.

4. Terzan 1: the cluster Colour-Magnitude diagram and luminosity function

4.1. The Colour-Magnitude diagram

Figs. 2 shows the V vs. $(V-I)$ CMDs for the individual WFPC chips, as well as the combined diagram from all three chips. All CMDs show essentially the same features. However, Figs. 2b and 2c contain a relatively higher proportion of field stars as compared to Fig. 2a, since W2 and W4 are offset relative to the cluster center.

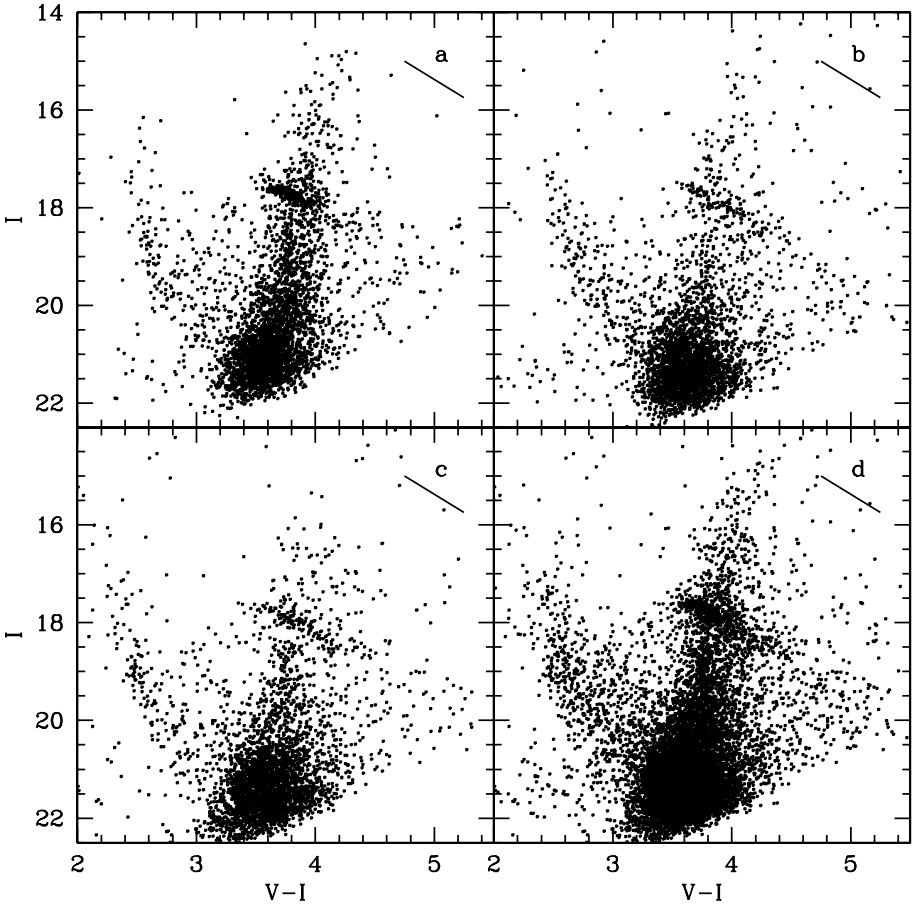

Fig. 3a–d. I vs. (V-I) CMDs for **a** W3; **b** W2; **c** W4; **d** W2+W3+W4.

In Figs. 3 the I vs. $(V-I)$ CMDs are given for the same sequence of chips given in Figs. 2.

4.2. The horizontal branch

As shown in Figs. 2 and 3, the cluster has a populous, very red HB located at V_{HB} = 21.4±0.1, and I_{HB} = 17.7±0.1. This HB morphology is typical of high-metallicity clusters such as e.g. NGC 6553 and NGC 6528 (Ortolani et al. 1995). The red HB is elongated and tilted, mostly due to differential reddening as indicated by being nearly parallel to the reddening line shown in the various CMDs. The differential reddening is more pronounced in Fig. 2b (W2) showing $\Delta(V-I) \approx 1.0$, from the extent of the red HB and the width of the RGB.

It is important to establish whether the HB tilt is entirely due to differential reddening, or whether there is an intrinsic contribution to the tilt. For example, Sweigart & Catelan (1998) were able to produce tilted red HBs resulting from differential helium enrichment due to mixing during the red giant branch (RGB) phase. In a central extraction ($r < 10''$) shown in Fig. 4b the HB tilt remains, suggesting that part of the tilt may be intrinsic, or alternatively to very small-scale differential reddening. We performed several tests with small extraction to check this point. The comparison of individual 8″ square boxes shows that differential absorptions up to $A_V = 0.2$ mag are still present also at this scale. The observed tilt of the HB $\Delta V/\Delta(V-I) = 2.0\pm0.2$ is in good agreement with the value expected from interstellar reddening alone in the WFPC2 system, which is 2.5.

4.3. The red giant branch

The previous ground-based CMD (Ortolani et al. 1993a) reached the RGB and the HB to the limiting magnitude $V \approx 22$. The HST CMD goes ~ 3 magnitudes deeper, and the turnoff is reached near the limit. Figs. 2 show a fairly steep RGB, resembling that of the metal poor globular clusters such as M30 or NGC 6752 ([Fe/H] = -2.13 and -1.54 respectively, Zinn & West 1984) (e.g. Rosino et al. 1997). The steepness of the RGB is especially evident in Fig. 4b, with the central extraction ($r < 10''$) virtually eliminating the foreground/background contamination.

This steep RGB is at odd with the red HB of the cluster. In Fig. 5 we overlap to the cluster CMD (from W3 with $r < 40''$) the mean locus of the metal-rich cluster NGC 6553 (Ortolani et al. 1995, Guarnieri et al. 1998), and that of globular cluster NGC 362 ([Fe/H] = -1.27, Zinn & West 1984; [Fe/H] = -1.16, Harris 1996), a well known *second parameter* cluster (e.g., Bolte 1989). The mean locus line of NGC 362 was obtained from Rosenberg et al. (1999). This comparison shows that the main features of Terzan 1 (SGB, HB, GB), even if Terzan 1 appears a bit more extreme case of a second parameter effect, with a somewhat steeper GB and a slightly redder HB.

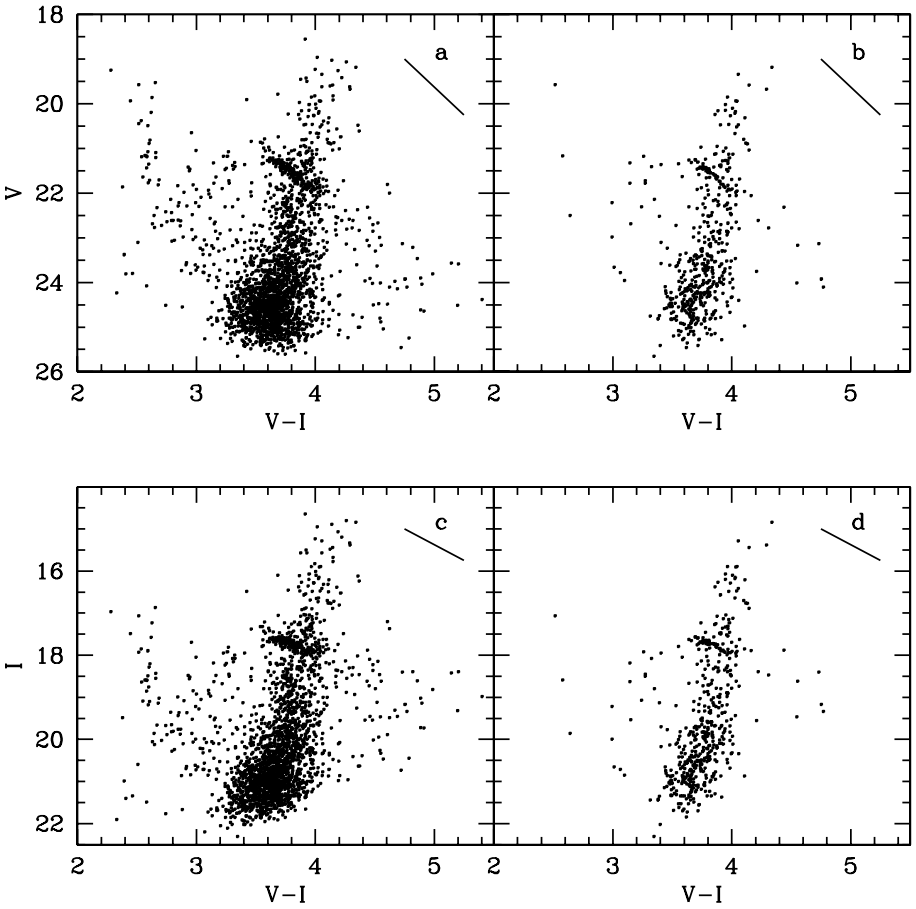

Fig. 4a–d. Extraction of the central part of the cluster in W3: **a** r $< 40''$ in V vs. V-I; **b** r $< 10''$ in V vs. V-I; **c** r $< 40''$ in I vs. V-I; **d** r $< 10''$ in I vs. V-I

4.4. The population of the main branches and the Helium abundance

Star counts in the W3 frame were carried out in order to check the radial distribution of the main CMD sequences, to verify cluster membership and field contamination, and to compute the ratios between different evolutionary phases. In Table 3 we show the counts for total field, a square containing the cluster center with ($X, Y <$ 300 pixels) and another square of equal area at the opposite edge of the field (500 $< X, Y <$ 800 pixels). The features were selected in the I vs. $(V - I)$ diagram. The CMD boxes containing the various sequences were defined as follows: (i) the RGB above the red HB: $I < 17.5$; $3.7 < (V - I) < 4.5$; (ii) the HB: $17.4 > I > 18.0$; $3.6 < (V - I) < 4.1$; and (iii) a control region containing the disk main sequence (MS): $I < 19.6$; $(V - I) < 2.9$.

Note that the counts in the disk MS scales with the area, as expected from a uniform field distribution, while there is a clear concentration of the RGB and the red HB towards the cluster center, showing that the vast majority of the stars in these features belong to the cluster. We also took into account a correction for the RGB stars included within the red HB box. The corrected counts for the cluster center area are indicated in parentheses in Table 3. The RGB correction for field contamination is negligible, but that for the RGB contamination of the red HB box is fairly large (31 stars), while the field correction amounts to 10 stars. The resulting ratio R' = HB/(RGB+AGB) = 1.11 implies a helium abundance $Y \simeq 0.23$ (Buzzoni et al. 1983).

Table 3. Star Counts in the W3 Field

zone	RGB	red HB	disk MS
Counts in I :			
whole frame	152	233	102
cluster center	82(81)	131(90)	12
frame edge	6	10	10

Note: Values in parentheses are corrected – see text

Note that the superior quality of the HST data and resulting CMD allows us to correct some misinterpretation of the CMD of Terzan 1 derived from our previous ground based observations (Ortolani et al. 1993a). The main advantage of the new HST data is that they allow to obtain accurate photometry down to the center of the cluster, where field contamination is much smaller than in the area explored from the ground. Fig. 3c in Ortolani et al. (1993a) showed only the RGB stars brighter than I $\approx$ 17, with an apparent clump of stars at $I = 15.95$ that we interpreted as the HB clump. The HST data (Fig. 4d) show instead that the HB clump is at $I = 17.7$, which also reveals very clearly the steep RGB that could not be identified on the ground-based CMD due to the incorrect placement of the HB and to the extensive contamination by bulge field RGB stars.

Therefore, the key advantage of the present data is that the HST high resolution permits to reach deeper magnitudes in the central area. The difference is not due to the higher photometric accuracy per se, as can be checked by a comparison of Fig. 3a in Ortolani et al. (1993a) with Fig. 3d of the present paper. These figures correspond to 12 arcmin^2 and 6.7 arcmin^2 respectively, and show that the width of the giant branch brighter than the HB is quite the same in both cases, because it is dominated by field contamination and differential reddening rather than by the photometric accuracy.

4.5. Reddening and distance

The correct procedure to obtain the $E(B-V)$ and the $A_{\rm V}$ is to use the coefficients provided by Holtzman et al. (1995) for the WFPC2 instead of the Dean et al. (1978) values which were derived for standard Johnson-Cousins passbands. This is a consequence of the different width, effective wavelength and shape between the WFPC2 and Johnson-Cousins system which cannot be accounted for by the colour transformation. In principle this calculation should be done on the original instrumental magnitudes, but, as we already mentioned in Sect. 3, the colour term transformations from F555W magnitudes to the V band and from F814W to the I band are so small that the numerical difference in the reddening calculations is practically negligible being of the order of a few hundredths of a magnitude. However, for a high reddening, the correct choice of the reddening law is crucial. In particular, in our case, it must take into account the systematically bluer passbands of the WFPC2 system. Using throughout the paper the ratio $E(V-I)/E(B-V)$ = 1.19 (Holtzman et al. 1995,) one obtains $E(B-V)$ = 2.28, close to the highest value listed in Table 2. Assuming R = $A_{\rm V}$/E(V-I) = 2.51 recommended for HST filters, we obtain $A_{\rm V}$ = 6.78.

We first calculate the cluster reddening differentially with respect to the metal-rich template NGC 6553. By superimposing the red HB of the two clusters one gets $\Delta(V-I) = 1.75 \pm 0.08$ between Terzan 1 and NGC 6553. Adopting $E(V-I) = 0.95$ for NGC 6553 (Guarnieri et al. 1998), one obtains $E(V-I) = 2.70$ for Terzan 1. The red HB level in Terzan 1 is at $V_{\rm HB}$= 21.4±0.1. Adopting an absolute magnitude $M_{\rm V}$ = 0.94 for a metal-rich cluster (Guarnieri et al. 1998), and with $A_{\rm V}$ = 6.78 the absolute distance modulus is $(m-M)_\circ = 13.68 \pm 0.15$, which leads to a distance from the Sun $d_\odot = 5.4 \pm 0.5$ kpc for Terzan 1.

Alternatively, on the other extreme, one can assume the very metal poor cluster M30 as a template. Matching to each other the steep RGBs of the two clusters, we obtain $\Delta(V-I) = 2.95 \pm 0.08$ between Terzan 1 and M30. Adopting $E(B-V) = 0.03$ for M30 (Harris 1996), we get $E(V-I) = 2.99$, which converts into $E(B-V) = 2.48$ for Terzan 1, and corresponds to $A_{\rm V}$ = 7.43.

With $V_{\rm HB}$ = 21.4 for Terzan 1, and adopting an absolute magnitude $M_{\rm V}$ = 0.45 (Buonanno et al. 1989) for M30, the absolute distance modulus is $(m-M)_\circ = 13.52 \pm 0.15$, which leads to a distance from the Sun $d_\odot = 5.05 \pm 0.5$ kpc for Terzan 1. Using instead NGC 362 as a template intermediate values are obtained. Despite the fact that the two templates have different morphologies and metallicities, the reddening and distances are very similar in the two derivations. Let us note that the distance derived by Ortolani et al. (1993a) for Terzan 1 was considerably closer to the Sun, because the HB was placed too bright, due to the lower photometric accuracy caused by crowding in those early ground-based observations.

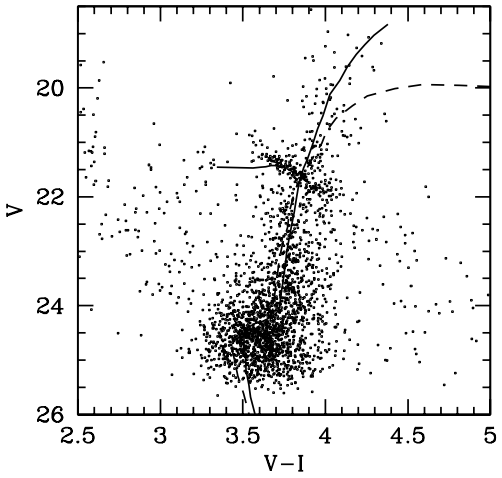

Fig. 5. W3 V vs. (V-I) diagram for an extraction of r $< 40''$ where mean loci of NGC 6553 (dash-dotted line) and NGC 362 (solid line) are superimposed.

Adopting a mean distance of 5.2 kpc for Terzan 1, and assuming the distance of the Galaxy center of $R_\odot$ = 8.0 kpc (Reid 1993), the Galactocentric coordinates of Terzan 1 are $X = -2.8$ (X <0 refers to our side of the Galaxy), $Y = -0.4$ and $Z = 0.1$ kpc. With a galactocentric distance of ~ 2.8 kpc Terzan 1 is thus located well inside the bulge. In this regard see also the recently derived spatial distribution of the bulge globular clusters in Barbuy et al. (1998).

It must be pointed out, however, that the distance is very dependent on the choice of the selective-to-total absorption R. If we assume, for example, E(V-I)/E(B-V) = 1.33 (Dean et al. 1978) and $A_{\rm V}$/E(B-V) = 3.1, we obtain 6.5 kpc.

4.6. The luminosity function

Fig. 6 shows the I-band luminosity function of Terzan 1 derived from W2 camera in an attempt to compromise between the crowding and the contamination from the field, compared with that obtained from NGC 362 (Rosenberg et al. 1999). Only the stars closer than 35″ from the Terzan 1 center have been included. The luminosity function of NGC 362 has been normalized to Terzan 1 scaling to the same number of stars in the horizontal branch. It has been also shifted in magnitude in order to overlap the two HBs. From the comparison the good agreement between the two luminosity functions is evident from the HB, along the SGB, until the turnoff region. In NGC 362 the turnoff is located at about 3.1 mag. below the HB, which corresponds to about $I = 21$ in Fig. 6 (which is scaled to Terzan 1).

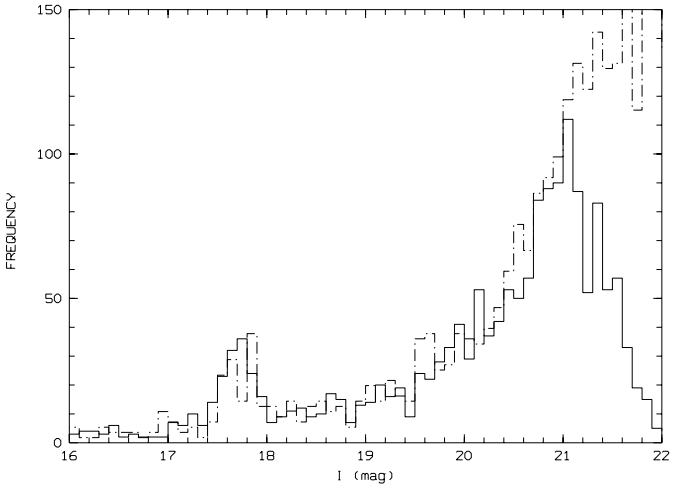

Fig. 6. I luminosity functions of Terzan 1 (solid line) and NGC 362 (dashed line).

This is also the photometry limit in Terzan 1, with a sharp drop in the completeness at fainter magnitudes.

Given the uncertainties involved at the photometric limit (spurious detections, contaminations, completeness, bias in the magnitude of the faintest stars) a precise age cannot be inferred. However this comparison could be considered as an indication of a comparable age between the two clusters.

5. Discussion

We have presented HST/WFPC2 Colour-Magnitude Diagrams of Terzan 1 showing a puzzling combination of a steep RGB together with a dominant red HB. We have also shown that both the CMD and the LF of Terzan 1 are very well fit by their analogs for the classical second parameter cluster NGC 362. The most straightforward interpretation is therefore that both the metallicity and age of the two clusters are very similar.

As far as the metallicity is concerned, this conclusion ([Fe/H]$\simeq -1.2$) is at variance with previous attempts based on integrated photometry and spectrophotometry of the cluster, and calls for high-resolution spectroscopy of individual cluster stars for a confirmation. The high degree of contamination from the disk+bulge field, and perhaps even by captured stars (Bica et al. 1997), could account for the discrepant value of the metallicity indicated by integrated light studies. A few low-resolution spectra of individual stars of Terzan 1 are now available (Idiart et al. 1999), which should allow one to have a more direct estimate of its metallicity and radial velocities of individual stars.

Concerning the age, following Bolte's (1989) reasoning for NGC 362, also Terzan 1 should be a few Gyr younger than a cluster such as NGC 288 which has nearly the same metallicity but an extended, very blue HB. As such, Terzan 1 appears to be a second parameter cluster physically located within the Galactic bulge. Since its tangential velocity is not known, it is at this stage impossible to say whether Terzan 1 is a genuine bulge cluster, or a halo cluster that happens to be crossing through the bulge at this particular epoch.

Rich et al. (1997) discovered two second parameter clusters in the Galactic bulge, NGC 6441 and NGC 6388. They are both metal rich clusters with a composite HB, with both red and blue stars. Terzan 1 represents the opposite case of a second parameter effect, i.e., a fairly metal-poor cluster with an almost purely red HB, a case also similar to the globular cluster No. 1 in the Fornax dwarf spheroidal (Smith et al. 1998), which however appears to have within ± 1 Gyr the same age of the other three clusters with blue HBs (Buonanno et al. 1998).

Acknowledgements. We thank Giampaolo Piotto for having provided us the NGC 362 data before publication. We are also very grateful to Manuela Zoccali for the help in preparing the figures. BB and EB acknowledge partial financial support from CNPq and Fapesp.

References

Armandroff T.E, Zinn R., 1988, AJ 96, 92
Barbuy B., Bica E., Ortolani S., 1998, A&A 333, 117
Bica E., Barbuy B., Ortolani S., 1993, ApJ 382, L15
Bica E., Clariá J.J., Piatti A.E., Bonatto C., 1998, A&AS 131, 483
Bica E., Dottori H., Rodrigues I.O.F., Ortolani S., Barbuy B., 1997, ApJ 482, L49
Bolte M., 1989, AJ 97, 1688
Buonanno R., Corsi C.E., Fusi Pecci F., 1989, A&A 216, 80
Buonanno R., Corsi C., Zinn R., et al., 1998, ApJ 501, L33
Buzzoni A., Fusi-Pecci F., Buonanno R., Corsi C.E., 1983, A&A 128, 94
Dean J.F., Warpen P.R., Cousins A.J., 1978, MNRAS 183, 569
Guarnieri M.D., Ortolani S., Montegriffo P., et al., 1998, A&A 331, 70
Harris W.E., 1996, AJ 112, 1487
Holtzman J.A., Burrows C.J., Casertano S., et al., 1995, 107, 1065
Idiart T., Barbuy B., Perrin M.-N., et al., 1999, in preparation
Lee Y.-W., Demarque P., Zinn R.J., 1994, ApJ 423, 248
Malkan M.A., 1982, In: Philip A.G.D., Hayes D.S. (eds.) Astrophysical parameters for globular clusters. Davis Press, Schenectady, 533
Minniti D., 1995, AJ 109, 1663
Origlia L., Ferraro F.R., Fusi Pecci F., Oliva E., 1997, A&A 321, 859
Ortolani S., Barbuy B., Bica E., 1991, A&A 249, L31
Ortolani S., Bica E., Barbuy, B., 1993a, A&A 267, 66
Ortolani S., Bica E., Barbuy B., 1993b, ApJ 408, L29
Ortolani S., Renzini A., Gilmozzi R., et al., 1995, Nat 377, 701
Peterson C., 1993,In: Djorgovski S., Meylan G. (eds.) ASP Conf. 50, p. 337
Reid M., 1993, ARA&A 31, 345
Rich R.M., Craig S., Djergovski S.G., Piotto G., King I.R., et al., 1997, ApJ 484, L25
Rosenberg A., Piotto G., Saviane I., Aparicio A., 1999, A&AS submitted
Rosino L., Ortolani S., Barbuy B., Bica E., 1997, MNRAS 289, 745
Smith E.O., Rich R.M., Neill J.D., 1998, AJ 115, 2369
Sweigart A.V., Catelan M., 1998, ApJ 501, L63
Terzan A., 1968, C. R. Acad. Sci. Paris 267, 1245
Trager S.C., King I.R., Djorgovski S., 1995, AJ 109, 218
Webbink R.F., 1985, In: Goodman J., Hut P. (eds.) Dynamics of Star Clusters. IAU Symp. 113, Reidel, Dordrecht, p. 541
Zinn R., West M.J., 1984, ApJS 55, 45